



Published in final edited form as:

Mech Dev. 2009 ; 126(3-4): 212. doi:10.1016/j.mod.2008.11.002.

A neural crest deficit in Down syndrome mice is associated with deficient mitotic response to Sonic hedgehog

Randall J. Roper^{1,2,4}, Justin F. VanHorn², Colyn C. Cain³, and Roger H. Reeves^{1,4}

¹ Department of Physiology and McKusick-Nathans Institute for Genetic Medicine, Johns Hopkins University School of Medicine, Baltimore, MD 21205, USA

² Department of Biology and Indiana University Center for Regenerative Biology and Medicine, Indiana University-Purdue University Indianapolis, Indianapolis, IN 46202, USA

³ Department of Gynecology and Obstetrics, Johns Hopkins University School of Medicine, Baltimore, MD 21205 USA

Abstract

Trisomy 21 results in phenotypes collectively referred to as Down syndrome (DS) including characteristic facial dysmorphology. Ts65Dn mice are trisomic for orthologs of about half of the genes found on human chromosome 21 and exhibit DS-like craniofacial abnormalities, including a small dysmorphic mandible. Quantitative analysis of neural crest (NC) progenitors of the mandible revealed a paucity of NC and a smaller first pharyngeal arch (PA1) in Ts65Dn as compared to euploid embryos. Similar effects in PA2 suggest that trisomy causes a neurocristopathy in Ts65Dn mice (and by extension, DS). Further analyses demonstrated deficits in delamination, migration, and mitosis of trisomic NC. Addition of Sonic hedgehog (Shh) growth factor to trisomic cells from PA1 increased cell number to the same level as untreated control cells. Combined with previous demonstrations of a deficit in mitogenic response to Shh by trisomic cerebellar granule cell precursors, these results implicate common cellular and molecular bases of multiple DS phenotypes.

Keywords

Trisomy 21; Down syndrome; neural crest; Sonic hedgehog; mandibular development

1. Introduction

Trisomy 21 (Down syndrome, DS) is the most common human aneuploidy compatible with survival and occurs in approximately 1 out of 700 live births (Christianson *et al.* 2006). Individuals with DS present with subsets of a wide range of clinical phenotypes including cognitive impairment, craniofacial dysmorphology, congenital heart defects, and gastrointestinal tract abnormalities. The presence or absence (penetrance) and severity (expressivity) of these features varies among individuals with trisomy 21, particularly in

4Corresponding authors: Randall J. Roper, Ph.D., Department of Biology, Center for Regenerative Biology and Medicine, Indiana University-Purdue University Indianapolis, 723 W. Michigan Street, SL 306, Indianapolis, IN 46202, Phone: 317-274-8131, Fax: 317-274-2846, rjroper@iupui.edu, Roger H. Reeves, Ph.D., Department of Physiology and McKusick-Nathans Institute for Genetic Medicine, Johns Hopkins University School of Medicine, Biophysics 201 725 North Wolfe Street, Baltimore, MD 21025, Phone: 410-955-6621, Fax: 443-287-0508, rreeves@jhmi.edu.

Publisher's Disclaimer: This is a PDF file of an unedited manuscript that has been accepted for publication. As a service to our customers we are providing this early version of the manuscript. The manuscript will undergo copyediting, typesetting, and review of the resulting proof before it is published in its final citable form. Please note that during the production process errors may be discovered which could affect the content, and all legal disclaimers that apply to the journal pertain.

cardiac and gastrointestinal systems which are frequently not affected in people with DS (Epstein 2001; Van Cleve *et al.* 2006; Van Cleve and Cohen 2006). Craniofacial anomalies are common to all individuals with DS and persist from early prenatal through postnatal and adult stages (Allanson *et al.* 1993; Guihard-Costa *et al.* 2006). Characteristic DS facial features include both skeletal abnormalities (shortened midface and small mandible and oral cavity) and soft tissue abnormalities (upsloping palpebral fissures, inner epicanthic folds) (Epstein 2001). Other DS phenotypes may result secondarily from primary craniofacial structural abnormalities including macroglossia and tongue hyperprotrusion, impaired mastication and speech, narrow airways, dental anomalies, chronic ear disease and hearing loss, recurrent illness and sleep apnea (Shott 2006; Venail *et al.* 2004). Formation of the face requires the integrated development of a variety of tissue and cell types so that a miscue in any of these developmental processes as a consequence of trisomy 21 may affect multiple attributes of craniofacial structure and function (Helms and Schneider 2003; Knight and Schilling 2006).

Mouse models have been used to investigate the incidence and severity of a number of DS phenotypes (Dierssen *et al.* 2001; Moore and Roper 2007). The best characterized mouse model of DS is the Ts(17¹⁶)65Dn mouse (hereafter Ts65Dn). This segmental trisomy model carries a small translocation chromosome comprised of the distal region of Mmu16 attached to the centromeric end of Mmu17 (Reeves *et al.* 1995) and contains orthologs of about half of the genes on human chromosome 21 (Hsa21) (Gardiner *et al.* 2003; Hattori *et al.* 2000). Precise quantitative measurements of Ts65Dn mice found alterations in skull morphology corresponding to those observed in individuals with DS (Richtsmeier *et al.* 2000; Richtsmeier *et al.* 2002). At birth, Ts65Dn mice show differences in the anterior face, anterior and posterior neurocranium, palate, and mandible compared to euploid littermates (Hill *et al.* 2007). Analysis of postnatal growth patterns showed that most alterations in craniofacial structure are apparent in newborn trisomic mice and predict the dysmorphology of adult stages, suggesting that alterations in the early development of the craniofacial skeleton are a major factor in forming the characteristic DS facial phenotype.

Neural crest (NC) contribute to the majority of the bone, cartilage, connective tissue and peripheral nervous tissue in the head (Santagati and Rijli 2003). The correct formation of the craniofacial skeleton is necessary for the proper development of the brain, sensory organs, and the normal functioning of the digestive and respiratory tracts (Le Douarin *et al.* 2007; Santagati and Rijli 2003). Besides craniofacial and neurological abnormalities, other NC-derived tissues possibly disrupted by trisomy include the sensory and autonomic (e.g. enteric ganglia) nervous systems, tongue, and developing heart. Because NC is a common precursor of many structures affected in DS, it has been hypothesized that trisomy 21 affects NC, though no direct experimental evidence supports or refutes this hypothesis (Johnston and Bronsky 1991; Kirby 1991; Yamakawa *et al.* 1998). Increased expression of a gene or genes on Hsa21 could affect subsets of NC during development by altering intrinsic and/or extrinsic signaling involved in NC programming (Potier *et al.* 2006; Roper and Reeves 2006).

Induction, delamination, migration and proliferation of NC are influenced by a number of morphogens and transcription factors and involve signals from multiple embryonic tissues (Knight and Schilling 2006). Among these, Shh was of particular interest given the recent demonstration of an attenuated mitogenic response to Shh by trisomic granule cell precursors from the developing cerebellum (Roper *et al.* 2006a). Targeted disruption of Shh in mice also causes defects in the developing neural tube, abnormal migration of NC, and a hypoplastic PA1 with fewer proliferating NC (Jeong *et al.* 2004; Washington Smoak *et al.* 2005; Yamagishi *et al.* 2006). Because of the very wide range of processes affected by Shh, a generalized attenuation of the response to Shh by trisomic cells could contribute to multiple DS phenotypes. Here we demonstrate both NC and Shh response deficits that may represent cellular and

molecular “common denominators” of pathogenesis contributing to multiple aspects of the trisomic phenotype in DS.

2. Results and Discussion

2.1 Neural crest deficit in Ts65Dn mice

Neural crest (NC) induction occurs at the neural plate border with delamination from the neural tube followed by migration at distinct axial levels within the developing embryo. During this process, NC identity, migration and proliferation are influenced by intrinsic programming as well as by external signals (Knight and Schilling 2006). Streams of NC populate craniofacial precursors including the 1st pharyngeal arch (PA1), and contribute to the skeleton of the mid- and lower face. In particular, NC within the mandibular component of PA1 become incorporated into the emergent mandible (Chai *et al.* 2000).

Ts65Dn mice and individuals with DS exhibit hypoplasia of the mandible and mid-facial skeleton (Richtsmeier *et al.* 2000). To characterize the possible role of NC on this process, we crossed Ts65Dn to mice expressing lacZ under control of the *Wnt1* promoter (Echelard *et al.* 1994). *Wnt1* expression is restricted to NC during migration and investment of PA1 and thus these cells can be identified by staining for lacZ. Embryos were recovered at E9.5 and staged according to paired somite number (Figure 1A-D). Trisomic and euploid embryos occur at the same frequency at E9.5 and have the same average number of somites (Roper *et al.* 2006b).

We isolated Theiler stage 15 (T15) embryos displaying 21-24 somites and performed stereological analysis to compare properties of trisomic and euploid embryos (see Methods). Although the overall size of euploid and trisomic embryos was similar at this stage, the volume of PA1 in trisomic embryos was significantly reduced to 81% of euploid ($p = 0.03$) (Table 1). Concomitant with the reduction of PA1 size, there were significantly fewer NC within PA1 of trisomic embryos compared to euploid (20,711 vs. 25,125, $p = 0.03$). The hyoid arch or PA2 was also reduced in size and contained fewer NC in Ts65Dn at this stage. When the PA1 or PA2 arch volume was normalized to embryo volume, trisomic PA1 and PA2 volume was significantly reduced as compared to euploid ($p = 0.01$ and 0.03 , respectively). Because trisomy affects NC in both PA1 and PA2, regions that contribute to different adult structures, it will be important to determine whether trisomy affects all axial and temporal NC subpopulations in the same way as facial skeletal NC precursors or if there are regional differences in response. Our results provide the first experimental evidence that trisomy for orthologs of about half of the conserved genes on Hsa21 results in a deficit of NC, and that the pathogenesis of the small mandible, previously characterized in postnatal and adult Ts65Dn mice, is recognizable at midgestation by changes in mandibular precursors.

2.2 Temporal and spatial origin of trisomic NC deficit

To understand when NC differences become significant in trisomic mice, we examined the pharyngeal arches and NC in Theiler stage 14 (T14) embryos with 16-18 somites. At this stage of development, no significant differences were observed between trisomic and euploid embryos in either the number of NC investing or volume of PA1 or PA2 (Table 2). Thus mandibular precursor differences become significant between T14 and T15. Next we determined the number of NC entering the pharyngeal arches. Migrating NC from rhombomeres 1 and 2 form the trigeminal stream, a region between the neural tube and PA1, and a portion of these cells migrate into PA1 (Figure 2A) (Depew 2002). When lacZ positive NC within the trigeminal stream were quantified in T14 embryos, significantly fewer NC were seen in Ts65Dn as compared to euploid embryos ($p = 0.05$; Figure 2C). This deficit is transient; the number of NC in the trigeminal stream at T15 was not significantly different. The reduced

number of NC entering PA1 at T14 is the first of three effects of trisomy that contribute to hypoplasia of the mandibular precursor seen at T15.

2.3 Reduction in NC delamination and migration from trisomic neural tube explants

The number of trisomic NC entering PA1 would be reduced if fewer NC were generated and/or if fewer migrated successfully in Ts65Dn as compared to euploid embryos. We examined these possibilities using cranial neural tube explants from T14 embryos (Chareonvit *et al.* 1997). Explants devoid of surface ectoderm were cultured for 12 hours and cells that migrated from the explant were recovered and quantified. Recovered cells were stained for lacZ expression and analyzed by FACS to discriminate between NC and other cell types (Figure 3A, B). Although there were no significant differences in sizes of the trisomic and euploid explants at 0 or 12 hours, significantly fewer total cells emanated from Ts65Dn as compared to euploid explants (Figure 3C, $p = 0.01$). Further, cells from trisomic explants included only 11% lacZ positive NC cells compared to 20% in euploid explants (19,771 vs. 43,879, $p < 0.001$).

Cells from trisomic explants also showed impaired migration as evidenced by the distances traveled and area covered by trisomic cells that left the explants (Figure 3D-F). The farthest linear distance covered by cells from the explants was significantly shorter in trisomic than in euploid from both the ventral and dorsal sides at the level of rhombomere 2 ($p = 0.002$ and $p = 0.03$, respectively; orientation determined with respect to how the explants situated in the embryo). Rhombomere 2 is a major source of NC that migrate into PA1. The area covered by cells from Ts65Dn explants was also reduced compared to euploid ($p = 0.07$, Figure 3D). These results demonstrate a second contribution to the NC deficit in trisomic mice. The significantly reduced number of NC in the trigeminal stream of trisomic T14 embryos begins with a reduction of NC formation possibly exacerbated by impaired migration.

2.4 Reduced NC proliferation in PA1 of trisomic embryos

Trisomy results in reduced proliferation (and not increased apoptosis) of neuronal precursors in both the cerebellum and hippocampus (Chakrabarti *et al.* 2007; Contestabile *et al.* 2007; Lorenzi and Reeves 2006; Roper *et al.* 2006a). Reduced NC generation and migration may be compounded by reduced mitosis or increased apoptosis in trisomic cells that populate PA1. When T15 embryos were sectioned and stained to mark mitotic and apoptotic cells, there were fewer mitotic NC in PA1 of Ts65Dn as compared to euploid embryos (6% vs. 8% of total neural crest, respectively; $p = 0.08$) (Figure 2B, D). Apoptotic cells were too few to enumerate in either genetic background.

Since the NC deficit in PA1 is pronounced by T15, we examined proliferation at T14. PA1 is comprised of 90-95% NC during early development (Zhao *et al.* 2006). We removed PA1 from T14 Ts65Dn and euploid embryos, triturated into a single cell suspension, and plated 2500 cells on fibronectin coated wells with serum free medium. After 12 hours of culture, the number of cells from trisomic PA1 was significantly less than euploid (Ts65Dn: 4213 vs. euploid: 5213, $p < 0.05$). The reduced proliferation of trisomic PA1 cells represents a third effect contributing to the paucity of NC in PA1 of T15 Ts65Dn embryos.

2.5 Altered response to Shh may be a common mechanism in multiple DS phenotypes

Sonic hedgehog (Shh) is a mitogen for a number of cell types, including NC in PA1 and granule cell precursors (gcp) in the cerebellum (Jeong *et al.* 2004; Wechsler-Reya and Scott 1999). Trisomic gcp demonstrate a significant deficit in the Shh-induced mitogenic response relative to euploid precursor cells, leading to the hypomorphic cerebellum characteristic of Ts65Dn mice and DS (Roper *et al.* 2006a). If all trisomic cells had this Shh response deficit, this could contribute to anomalies in any structure with a contribution from Shh-responsive cell

populations, including NC. Alterations in Shh signaling have been shown to change NC migration leading to craniofacial dysmorphology (cranial NC) and Hirschsprung's disease (truncal NC) in animal models of Bardet-Biedl syndrome (Tobin *et al.* 2008). There is no information about Shh levels in trisomic mice, much less the effective concentration at the receptors of respective cells.

To examine the Shh response in a more controlled condition, we isolated cells from PA1 of trisomic or euploid T14 embryos and cultured them for 12 hours in media containing 2, 4 or 8 $\mu\text{g/ml}$ of Shh. Trisomic cells showed a smaller increase in cell number than euploid at all concentrations of Shh, but addition of 4 $\mu\text{g/ml}$ of Shh increased cell number of trisomic PA1 cells to the same level as untreated euploid cells (Figure 2E). This response was concentration dependent, since addition of 2 or 8 $\mu\text{g/ml}$ of Shh did not increase cell number of either trisomic or euploid PA1 cells. These results suggest that the NC proliferative response in PA1 responds to specific concentrations of Shh, and that stimulation of the Shh pathway can overcome the mitogenic deficit in trisomic cells. Involvement of a mitogenic response deficit to Shh in both cerebellum and PA1 raises the possibility that there may be a common mechanism underlying these disparate trisomic phenotypes. This further implies that trisomy for one or more dosage sensitive genes found in three copies in Ts65Dn mice may influence the Shh proliferative response of both cerebellar precursors and NC (Roper and Reeves 2006).

We traced the robust mandibular phenotype of trisomy to the earliest developmental stage at which cellular deficits become evident, identified the cell types and processes that are affected and demonstrated an aberrant response to an important molecular signal (Shh). This is the first direct demonstration that trisomy adversely affects a specific population of NC and how that results in a neurocristopathy in DS. Investigation of trisomic NC deficits in the mandibular precursor provides an approach for understanding common mechanisms leading to multiple DS phenotypes. Characterization of “common denominators” that underlie multiple developmental anomalies in trisomy can provide potential targets for therapeutic intervention to ameliorate craniofacial and other anomalies in DS.

3. Experimental Procedures

4.1 Mice

Female B6EiC3Sn a/A-Ts(17¹⁶)65Dn (Ts65Dn) and female and male B6CBA-Tg(Wnt1-lacZ) 206Amc/J (Wnt1-lacZ) mice were purchased from The Jackson Laboratory (Bar Harbor, ME). Ts65Dn females used in this study were generated in our laboratories at the Johns Hopkins University School of Medicine and Indiana University-Purdue University Indianapolis by Ts65Dn \times B6C3F1 matings and identified by FISH genotyping (Moore *et al.* 1999). Wnt1-lacZ mice were brother-sister mated and mice homozygous for the Wnt1-lacZ transgene were identified and maintained in our colonies. Female Ts65Dn mice were bred to homozygous male Wnt1-lacZ mice and checked for vaginal plugs the morning after the mating, with 12:00 p.m. on the date of the plug identified as E0.5. Nine days after the plug was identified, Ts65Dn mothers were sacrificed and embryos removed for analysis. Embryos from 19 litters were staged according to somite numbers and ranged from presomite to 29 somites. All animal research was reviewed and approved by institutional animal use and care committees at Johns Hopkins University and Indiana University-Purdue University Indianapolis.

4.2 Genotyping of embryos

Yolk sacs were removed and typed by FISH. Briefly, the yolk sac was suspended in 37° C Dulbecco's PBS (Sigma St. Louis, MO), centrifuged and resuspended in collagenase (type X1-S, 1000 U/ml in HBSS, Sigma), and incubated for 30 min. at 37° C. After centrifugation and supernatant removal, yolk sac was incubated in 0.075 M KCl. After 30 min. of incubation, one

drop of 3:1 methanol:acetic acid fix was added, mixture was centrifuged, supernatant removed, and sample was stored in 3:1 methanol:acetic acid at 4° C. Sample was dropped on slides and genotyped by FISH as described (Moore *et al.* 1999).

4.3 Sectioned embryos

Embryos were dissected, washed in 0.1 M phosphate buffer, fixed in 0.2% gluteraldehyde with 5 mM EGTA and 2mM MgCl₂ in 0.1 phosphate butter for 15 min. at room temperature, washed three times for 5 min. each in wash buffer (2 mM MgCl₂, 0.02% Nonidet P-40 in 0.1 M phosphate buffer) and stained with 0.025% 5-bromo-4-chloro-3-indolyl-beta-D-galactopyranoside (X-gal) in 5mM potassium ferricyanide, 5 mM potassium ferrocyanide for 1 hour at 37° C. Embryos were washed in wash buffer and postfixed overnight in 4% paraformaldehyde at 4° C. After fixation embryos were dehydrated in increasing amounts of ethanol, cleared with xylenes, and infiltrated with paraplast. Embryos were serially sectioned parasagittally at 16 µm and counterstained with eosin. Embryos examining mitotic and apoptotic cells were processed as described above with the exception of X-gal staining, and sections stained with cresyl violet.

4.4 Quantification of neural crest using unbiased stereology

Unbiased stereology was performed according to established principles (Mouton 2002). Images were viewed using the Stereologer system and software (Systems Planning and Analysis, Inc., Alexandria, VA). Systematic random sampling using the optical “disector” [sic] methodology was used for enumeration of the cells and the Cavalieri-point counting method for obtaining volumes. Ten euploid and eight Ts65Dn 21-24 somite (E9.5 or Theiler stage 15) embryos were used to analyze NC and NC derived structures. For PA1, every third section, and for PA2, every second section with arch tissue was analyzed by stereology starting at a random start point. NC in PA1 and PA2 in 21-24 somite animals were counted in disectors spaced in intervals of 60 and 50 µm, respectively, with dimensions of 150 µm² area and 8 µm depth with a 2 µm guard height. Mitotic cells were counted in three euploid and five Ts65Dn E9.5 embryos in every other section containing PA1 with disectors spaced in intervals of 50 µm with dimensions of 600 µm² area and 8 µm depth with a 2 µm guard height. NC and NC-derived structures were quantified in seven euploid and six Ts65Dn 16-18 somite embryos. For PA1, PA2, and trigeminal crest, every other section was analyzed by stereology starting at a random start point. PA1 NC were enumerated in disectors spaced in intervals of 50 µm, and PA2 and trigeminal NC were counted in disectors spaced at 40 µm with the dimensions of the probe in all three cases of 150 µm² area and 8 µm depth with a 2 µm guard. For E9.5 and E9.25 PA1, PA2, and trigeminal NC volume, Cavalieri methodology was used with 1000 µm² area per point, and for total embryo volume, every fourth section was analyzed with disectors representing 8000 µm² area per point. Average CE for all volumes and counts was ≤ 0.10. Statistical differences were determined using a 1 tailed Student's t test.

4.5 Neural tube explants

E9.25 embryos were dissected into DMEM (Invitrogen) from Ts65Dn mothers, yolk sacs removed, and gross developmental stage measurements recorded with a Nikon Digital Sight Imager. In 12 euploid and nine Ts65Dn 16-18 somite embryos, non-neural tube tissue was removed from the ventral side of embryo. Embryos were incubated with 100 µl of 1 mg/ml dispase (Roche Diagnostics, Indianapolis, IN), and 250 µl DMEM was added after 5.5 minutes. At 10 minutes post incubation, 30G needles were used to separate the neural tube from surrounding tissue, and neural tube rostral to otic vesicle was cultured in 250 µl DMEM without serum with 1% penicillin-streptomycin (Invitrogen) in an 8 well fibronectin coated culture slide (Beckton Dickinson Labware, Bedford, MA). Explants were incubated at 5% CO₂ at 37° C for 12 hours. Digital images using a Nikon Digital Sight Imager were taken of the whole

embryo, and of the explant at 0 and 12 hours of culture. The Imager program was used to quantify area of the explant at 0 and 12 hours, the area of the cells around (but not including) the explant, and the linear distance from the approximate dorsal and ventral edge of rhombomere 2 to the edge of the migrating cells on the dorsal and ventral side of the embryo (orientation with respect to how the explant was removed from the embryo). Cells migrating from the neural tube were removed from the plate into a microcentrifuge tube, dispersed and quantified on a hemacytometer. Statistical differences were determined using a 1 tailed Student's t test.

4.6 FACS sorting of lacZ labeled neural crest

Fluorescein di- β -D-galactopyranoside (FDG) is specific for lacZ expressing cells (Zhao *et al.* 2006). To find percentage of lacZ labeled NC, cells were resuspended in DMEM to a concentration of 1×10^6 cells/ml and incubated at 37° C for 5 min. Cells were then mixed 1:1 with 2 mM FDG in water and incubated at 37° C for 1 min. After incubation, cells were diluted with 10 \times cold DMEM and placed on ice for 30-60 min. FACS was done on six euploid and five Ts65Dn samples at the Indiana University Simon Cancer Center Flow Cytometry Center. Autofluorescence of cultured cells was compensated using cells incubated with PBS, and FDG-positive and negative cells in each sample were sorted and counted. Number of lacZ positive cells was calculated by taking the average percentage of cells multiplied by the number of cells coming from culture. Statistical differences were determined using a 1 tailed Student's t test.

4.7 PA1 cell culture

PA1 were removed from five euploid and nine Ts65Dn E9.25 16-18 somite embryos and triturated to a single cell suspension and counted on a hemacytometer. Four wells of 2500 cells for each sample were plated in 250 μ l serum free DMEM with 1% penicillin-streptomycin in an 8 well fibronectin coated culture slide and incubated at 5% CO₂ at 37° C for 12 hours. The amino terminal peptide of recombinant mouse Shh (R&D Systems, Minneapolis, MN) was added to PA1 samples to a final concentration of 2, 4, or 8 μ g/ml. Cells were quantified at 0 and 12 h using a Nikon Digital Sight Imager to verify initial and quantify final cell number. Statistical differences were determined using a 1 tailed Student's t test.

Acknowledgments

We thank Joy Yang for guidance on embryo dissection and processing, Bill Pavan and Ling Hou for advice and instruction in preparation of neural tube explants, Gail Stetten, Joseph McMichael and Sarah South for assisting with the genotyping, and Molly Lange and Charlotte Eyring for help with sectioning and staining the embryos. Samantha Deitz provided stereological analysis of T15 migrating NC and Jared Allen assisted with the figures. This work was supported by Public Health Awards F32HD043614 (RJR) and HD038384 (RHR).

References

- Allanson JE, O'Hara P, Farkas LG, Nair RC. Anthropometric craniofacial pattern profiles in Down syndrome. *Am J Med Genet* 1993;47:748–752. [PubMed: 8267006]
- Chai Y, Jiang X, Ito Y, Bringas P Jr, Han J, et al. Fate of the mammalian cranial neural crest during tooth and mandibular morphogenesis. *Development* 2000;127:1671–1679. [PubMed: 10725243]
- Chakrabarti L, Galdzicki Z, Haydar TF. Defects in embryonic neurogenesis and initial synapse formation in the forebrain of the Ts65Dn mouse model of Down syndrome. *J Neurosci* 2007;27:11483–11495. [PubMed: 17959791]
- Chareonvit S, Osumi-Yamashita N, Ikeda M, Eto K. Murine forebrain and midbrain crest cells generate different characteristic derivatives in vitro. *Dev Growth Differ* 1997;39:493–503. [PubMed: 9352204]
- Christianson, A.; Howson, CP.; Modell, B. March of Dimes Global Report on Birth Defects: The Hidden Toll of Dying and Disabled Children. March of Dimes Birth Defects Foundation; White Plains, NY: 2006. p. 1-98.

- Contestabile A, Fila T, Ceccarelli C, Bonasoni P, Bonapace L, et al. Cell cycle alteration and decreased cell proliferation in the hippocampal dentate gyrus and in the neocortical germinal matrix of fetuses with Down syndrome and in Ts65Dn mice. *Hippocampus* 2007;17:665–678. [PubMed: 17546680]
- Depew, M.; Tucker, AS.; Sharpe, PT. *Craniofacial Development*. Academic Press; San Diego: 2002.
- Dierssen M, Fillat C, Crnic L, Arbones M, Florez J, et al. Murine models for Down syndrome. *Physiol Behav* 2001;73:859–871. [PubMed: 11566219]
- Echelard Y, Vassileva G, McMahan AP. Cis-acting regulatory sequences governing Wnt-1 expression in the developing mouse CNS. *Development* 1994;120:2213–2224. [PubMed: 7925022]
- Epstein, CJ. Down Syndrome (Trisomy 21). In: Scriver, CR.; Beaudet, AL.; Sly, WS.; Valle, D., editors. *The Metabolic & Molecular Bases of Inherited Disease*. McGraw-Hill; New York: 2001. p. 1223-1256.
- Gardiner K, Fortna A, Bechtel L, Davisson MT. Mouse models of Down syndrome: how useful can they be? Comparison of the gene content of human chromosome 21 with orthologous mouse genomic regions. *Gene* 2003;318:137–147. [PubMed: 14585506]
- Guihard-Costa AM, Khung S, Delbecq K, Menez F, Delezoide AL. Biometry of face and brain in fetuses with trisomy 21. *Pediatr Res* 2006;59:33–38. [PubMed: 16326987]
- Hattori M, Fujiyama A, Taylor TD, Watanabe H, Yada T, et al. The DNA sequence of human chromosome 21. *Nature* 2000;405:311–319. [PubMed: 10830953]
- Helms JA, Schneider RA. Cranial skeletal biology. *Nature* 2003;423:326–331. [PubMed: 12748650]
- Hill CA, Reeves RH, Richtsmeier JT. Effects of aneuploidy on skull growth in a mouse model of Down syndrome. *J Anat* 2007;210:394–405. [PubMed: 17428201]
- Jeong J, Mao J, Tenzen T, Kottmann AH, McMahon AP. Hedgehog signaling in the neural crest cells regulates the patterning and growth of facial primordia. *Genes Dev* 2004;18:937–951. [PubMed: 15107405]
- Johnston MC, Bronsky PT. Embryonic craniofacial development. *Prog Clin Biol Res* 1991;373:99–115. [PubMed: 1838193]
- Kirby ML. Neural crest and the morphogenesis of Down syndrome with special emphasis on cardiovascular development. *Prog Clin Biol Res* 1991;373:215–225. [PubMed: 1838187]
- Knight RD, Schilling TF. Cranial neural crest and development of the head skeleton. *Adv Exp Med Biol* 2006;589:120–133. [PubMed: 17076278]
- Le Douarin NM, Brito JM, Creuzet S. Role of the neural crest in face and brain development. *Brain Res Rev*. 2007
- Lorenzi HA, Reeves RH. Hippocampal hypocellularity in the Ts65Dn mouse originates early in development. *Brain Res* 2006;1104:153–159. [PubMed: 16828061]
- Moore CS, Lee JS, Birren B, Stetten G, Baxter LL, et al. Integration of cytogenetic with recombinational and physical maps of mouse chromosome 16. *Genomics* 1999;59:1–5. [PubMed: 10395793]
- Moore CS, Roper RJ. The power of comparative and developmental studies for mouse models of Down syndrome. *Mamm Genome* 2007;18:431–443. [PubMed: 17653795]
- Mouton, PR. *Principles and Practices of Unbiased Stereology: An Introduction for Bioscientists*. Johns Hopkins University Press; Baltimore: 2002.
- Potier MC, Rivals I, Mercier G, Ettwiller L, Moldrich RX, et al. Transcriptional disruptions in Down syndrome: a case study in the Ts1Cje mouse cerebellum during post-natal development. *J Neurochem* 2006;97:104–109. [PubMed: 16635258]
- Reeves RH, Irving NG, Moran TH, Wohn A, Kitt C, et al. A mouse model for Down syndrome exhibits learning and behaviour deficits. *Nat Genet* 1995;11:177–184. [PubMed: 7550346]
- Richtsmeier JT, Baxter LL, Reeves RH. Parallels of craniofacial maldevelopment in Down syndrome and Ts65Dn mice. *Dev Dyn* 2000;217:137–145. [PubMed: 10706138]
- Richtsmeier JT, Zumwalt A, Carlson EJ, Epstein CJ, Reeves RH. Craniofacial phenotypes in segmentally trisomic mouse models for Down syndrome. *Am J Med Genet* 2002;107:317–324. [PubMed: 11840489]
- Roper RJ, Baxter LL, Saran NG, Klinedinst DK, Beachy PA, et al. Defective cerebellar response to mitogenic Hedgehog signaling in Down [corrected] syndrome mice. *Proc Natl Acad Sci U S A* 2006a; 103:1452–1456. [PubMed: 16432181]

- Roper RJ, Reeves RH. Understanding the basis for Down syndrome phenotypes. *PLoS Genet* 2006;2:e50. [PubMed: 16596169]
- Roper RJ, St John HK, Philip J, Lawler A, Reeves RH. Perinatal loss of Ts65Dn Down syndrome mice. *Genetics* 2006b;172:437–443. [PubMed: 16172497]
- Santagati F, Rijli FM. Cranial neural crest and the building of the vertebrate head. *Nat Rev Neurosci* 2003;4:806–818. [PubMed: 14523380]
- Shott SR. Down syndrome: common otolaryngologic manifestations. *Am J Med Genet C Semin Med Genet* 2006;142:131–140. [PubMed: 16838306]
- Tobin JL, Di Franco M, Eichers E, May-Simera H, Garcia M, et al. Inhibition of neural crest migration underlies craniofacial dysmorphology and Hirschsprung's disease in Bardet-Biedl syndrome. *Proc Natl Acad Sci U S A* 2008;105:6714–6719. [PubMed: 18443298]
- Van Cleve SN, Cannon S, Cohen WI. Part II: Clinical Practice Guidelines for adolescents and young adults with Down Syndrome 12 to 21 Years. *J Pediatr Health Care* 2006;20:198–205. [PubMed: 16675381]
- Van Cleve SN, Cohen WI. Part I: clinical practice guidelines for children with Down syndrome from birth to 12 years. *J Pediatr Health Care* 2006;20:47–54. [PubMed: 16399479]
- Venail F, Gardiner Q, Mondain M. ENT and speech disorders in children with Down's syndrome: an overview of pathophysiology, clinical features, treatments, and current management. *Clin Pediatr (Phila)* 2004;43:783–791. [PubMed: 15583773]
- Washington Smoak I, Byrd NA, Abu-Issa R, Goddeeris MM, Anderson R, et al. Sonic hedgehog is required for cardiac outflow tract and neural crest cell development. *Dev Biol* 2005;283:357–372. [PubMed: 15936751]
- Wechsler-Reya RJ, Scott MP. Control of neuronal precursor proliferation in the cerebellum by Sonic Hedgehog. *Neuron* 1999;22:103–114. [PubMed: 10027293]
- Yamagishi C, Yamagishi H, Maeda J, Tsuchihashi T, Ivey K, et al. Sonic hedgehog is essential for first pharyngeal arch development. *Pediatr Res* 2006;59:349–354. [PubMed: 16492970]
- Yamakawa K, Huot YK, Haendelt MA, Hubert R, Chen XN, et al. DSCAM: a novel member of the immunoglobulin superfamily maps in a Down syndrome region and is involved in the development of the nervous system. *Hum Mol Genet* 1998;7:227–237. [PubMed: 9426258]
- Zhao H, Bringas P Jr, Chai Y. An in vitro model for characterizing the post-migratory cranial neural crest cells of the first branchial arch. *Dev Dyn* 2006;235:1433–1440. [PubMed: 16245337]

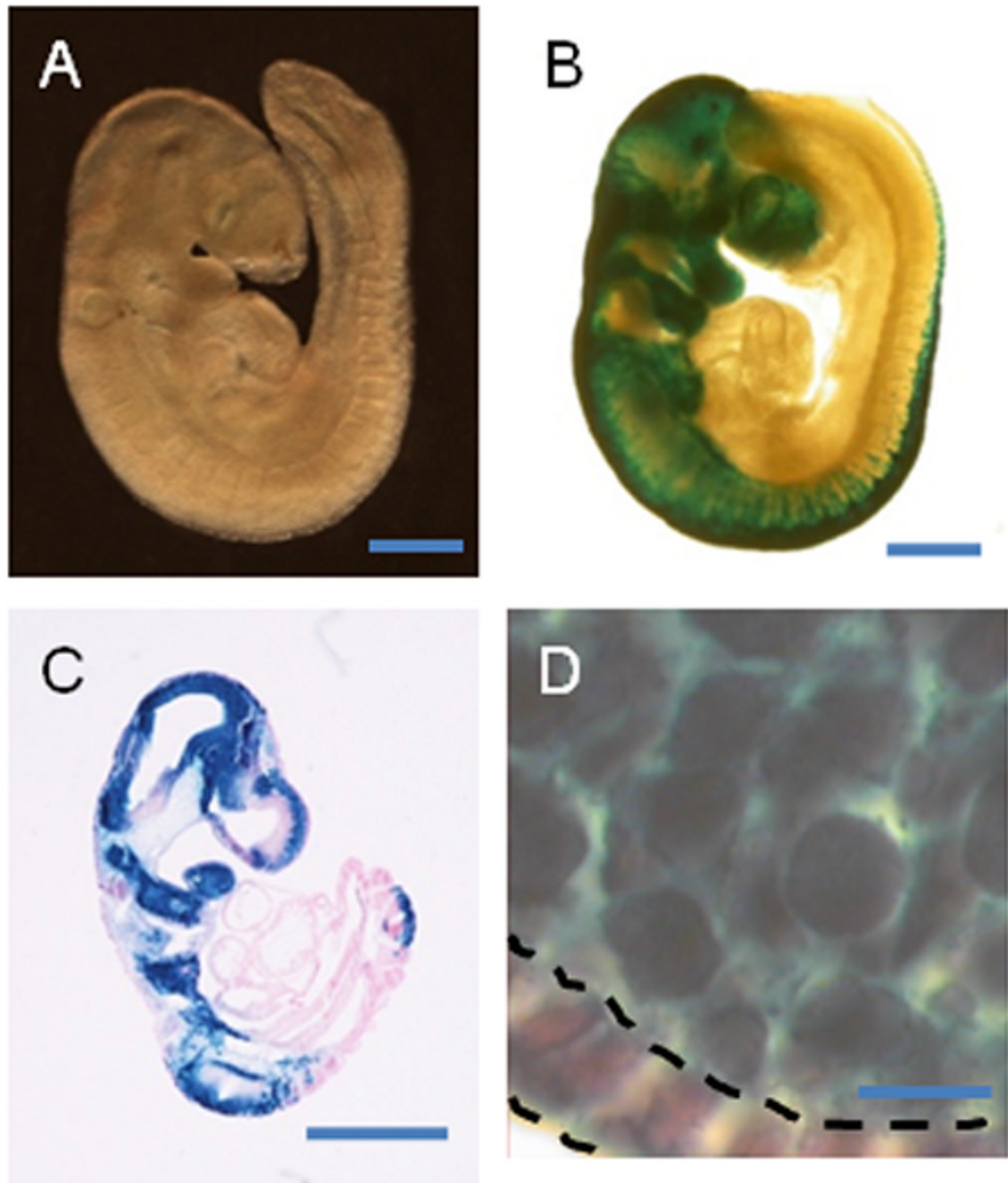


Figure 1.

Ts65Dn and euploid embryos with labeled NC. A., B. Euploid (A) and Ts65Dn, $Wnt1^{lacZ/+}$ (B) whole mount embryos show no gross morphological differences at T15 (22 somites)(see also Table 1). C. Parasagittal section of a T15 euploid embryo labeled with lacZ and counterstained with eosin. D. NC in the 1st pharyngeal arch stained with lacZ. LacZ staining of a thick (16 μ m) section labels NC but not endoderm (indicated by dashed lines). Scale bar in A-C is 500 μ m. Bar in D is 10 μ m.

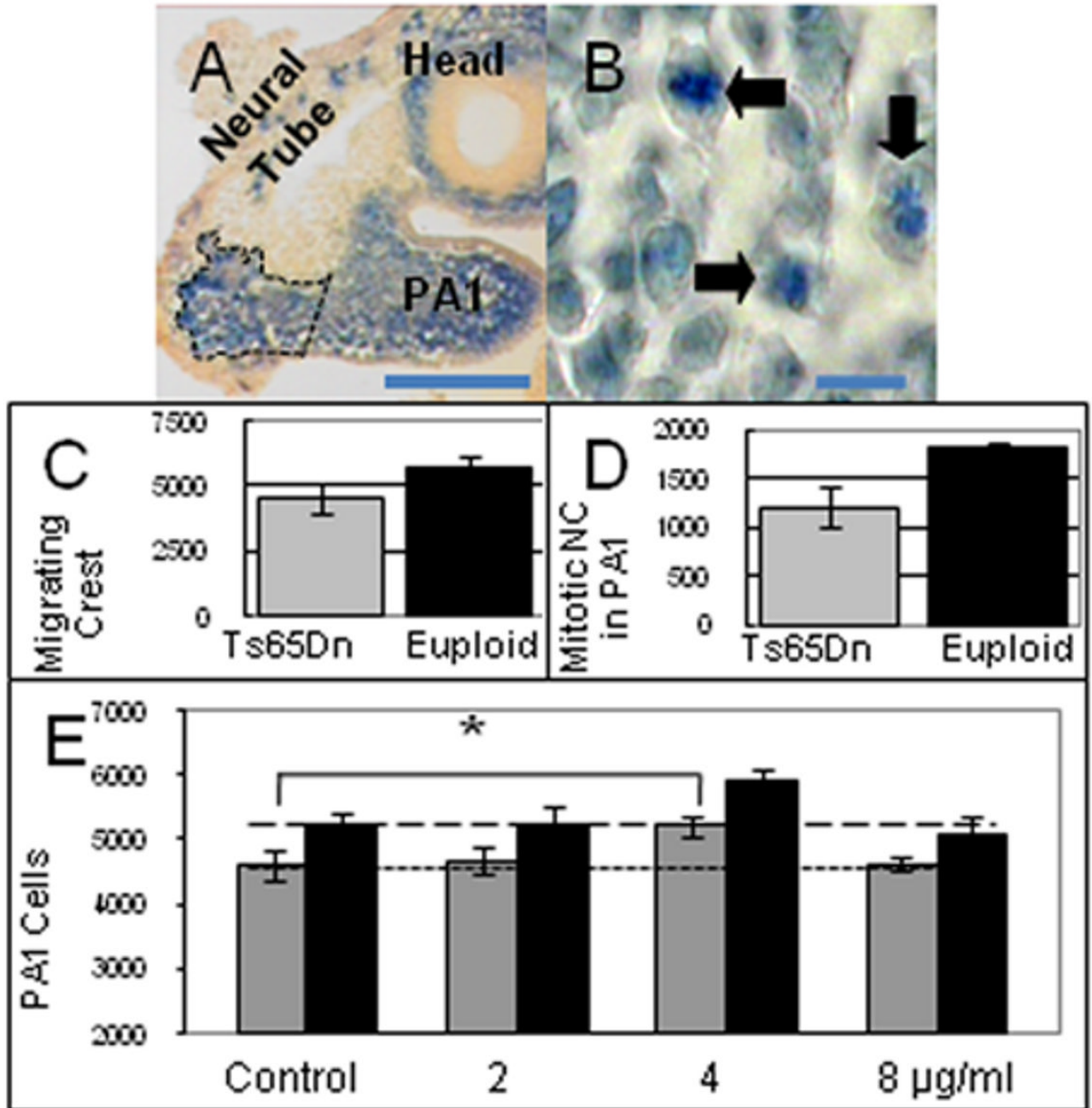


Figure 2.

Migration and proliferation of NC in trisomic mice. A. NC in the trigeminal stream between the neural tube and PA1 (outlined with broken line). Scale bar is 100 μ m. B. Mitotic cells in PA1 were identified by cresyl violet staining of thick sections (arrows). Scale bar is 10 μ m. C. The number of NC in the trigeminal stream of T14 Ts65Dn ($n = 5$) is significantly reduced relative to euploid ($n = 7$) ($p = 0.05$). D. The number of mitotic NC in PA1 of T15 Ts65Dn ($n = 5$) is reduced relative to euploid ($n = 3$) ($p = 0.07$). E. Effect of Shh on proliferation of PA1 cells. 2500 PA1 cells from each of nine Ts65Dn and five euploid T14 embryos were plated in culture dishes, incubated with or without Shh and the total cell number was determined after 12 hours. Trisomic (grey bars) PA1 cells proliferated significantly less than euploid (black

bars) at all concentrations of Shh after 12 hours in culture ($P < 0.05$ for control, 4 and 8 $\mu\text{g/ml}$; $p < 0.08$ for 2 $\mu\text{g/ml}$ Shh). Addition of 4 $\mu\text{g/ml}$ Shh to trisomic cells (third group) caused a significant increase in proliferation of trisomic cells, returning it to the level of proliferation seen in untreated euploid PA1 cells. * Statistically significant by Student's t test $p \leq 0.02$.

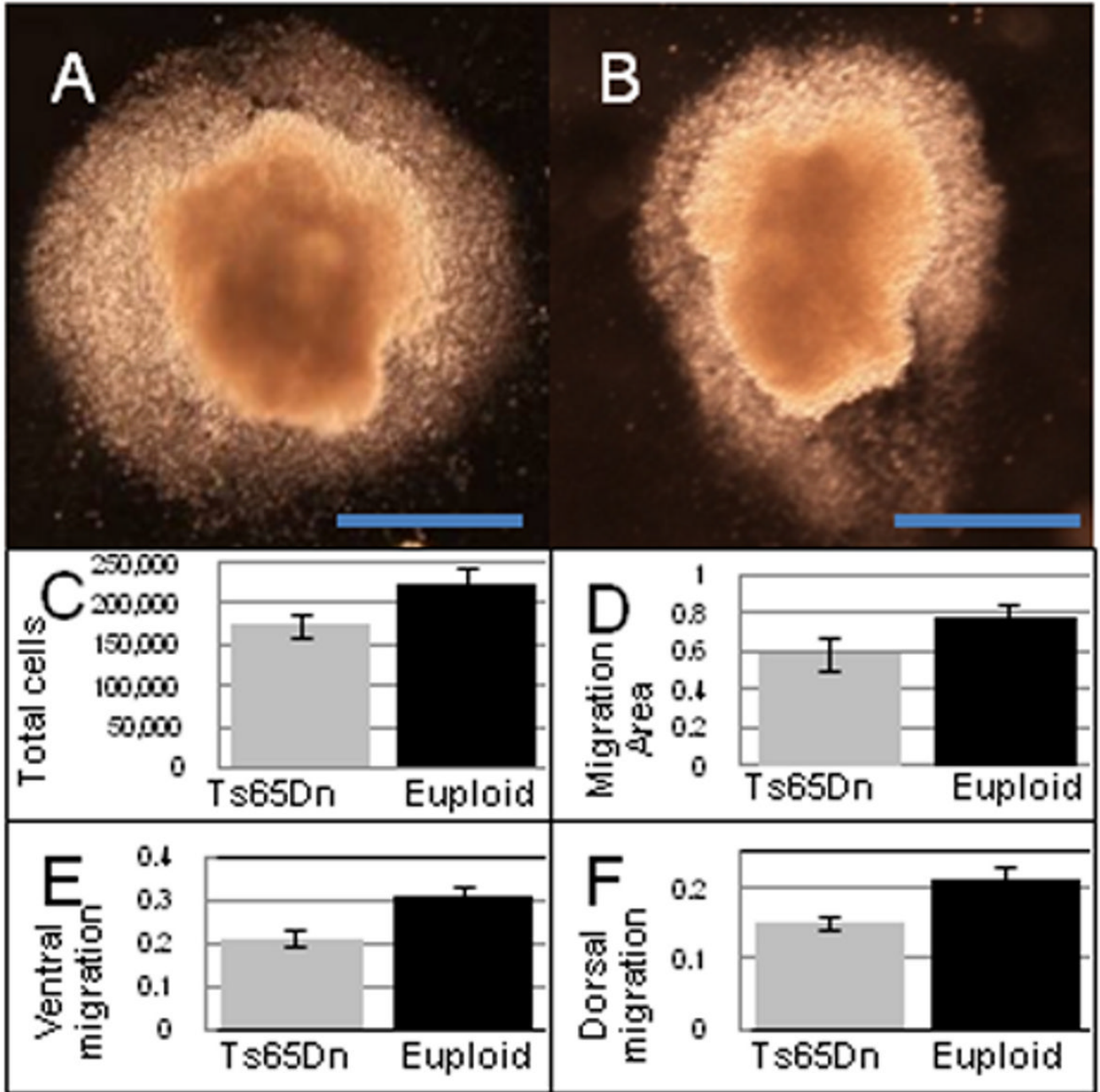


Figure 3. Neural tube explants. A., B. Cranial neural tube explants from 17 somite euploid (A) and trisomic (B) embryos after 12 hours of *in vitro* culture. The top is rostral (forebrain), bottom is caudal (hindbrain) and dorsal side is to the left. Total cellular migration area was delimited by the cells surrounding the explant and migration measured from the dorsal and ventral sides was at the approximate location of the second rhombomere (orientation with respect to how the explant was removed from the embryo). Scale bar = 500 μ m. C-F. Cell number and migration distances from trisomic (n = 9) and euploid (n = 12) T14 neural tube explants. Total cells migrating from (C) explants (p = 0.01), (D) area of migration (mm^2) around explants (p

= 0.07), (E) migration distance (mm) from ventral ($p = 0.002$), and (F) dorsal ($p = 0.03$) sides of explants are shown.

Table 1

PA-specific reductions in T15 Ts65Dn mice.

	N	Average Somites	Embryo Volume, μm^3	PA1 Volume, μm^3	PA1 Neural Crest	PA1 Neural Crest Density	PA2 Volume, μm^3	PA2 Neural Crest	PA2 Neural Crest Density
Euploid	10	22.4 (0.34)	5.82×10^8 (4.28×10^7)	1.34×10^7 (9.14×10^5)	25,125 (1,537)	1.89×10^{-3} (6.48×10^{-5})	5.61×10^6 (5.95×10^5)	10,807 (913)	1.97×10^{-3} (6.71×10^{-5})
Ts65Dn	8	22.4 (0.46)	5.45×10^8 (3.80×10^7)	1.09×10^7 (7.98×10^5)	20,711 (1,339)	1.94×10^{-3} (1.10×10^{-4})	4.20×10^6 (5.28×10^5)	8,495 (1,154)	2.02×10^{-3} (9.99×10^{-5})
Ts65Dn / Euploid		100%	94%	81%*	82%*	103%	75%*	79%**	102%

* Statistically significant by Student's t test, $p \leq 0.05$.

** Student's t test, $p = 0.07$.

Standard error of the mean in parentheses.

Table 2

No significant differences in PA between T14 Ts65Dn and euploid embryos.

	N	Average Somites	Embryo Volume, μm^3	PAI Volume, μm^3	PAI Neural Crest	PAI Neural Crest Density	PA2 Volume, μm^3	PA2 Neural Crest	PA2 Neural Crest Density
Euploid	7	17.4 (0.30)	3.11×10^8 (9.27×10^9)	4.86×10^6 (3.29×10^5)	11,832 (722)	2.49×10^{-3} (1.96×10^{-4})	1.86×10^6 (1.45×10^5)	4587 (368)	2.47×10^{-3} (6.64×10^{-5})
Ts65Dn	6	17.7 (0.31)	2.82×10^8 (1.69×10^7)	5.16×10^6 (4.21×10^5)	11,861 (862)	2.34×10^{-3} (1.70×10^{-4})	1.65×10^6 (1.71×10^5)	3939 (395)	2.44×10^{-3} (1.04×10^{-4})
Ts65Dn/Euploid		101%	91%	106%	100%	89%	89%	86%	99%